www.nesa-india.org • E-mail: nesapublications@gmail.com
International Journal on Environmental Sciences

International Journal on Environmental Sciences 13 (2) Pp. 89-98, ***July-December 2022***
ISSN No.: 0976-4534
https://doi.org/10.53390/ijes.v13i2.5

MONITORING AND SIMULATING LAND USE/COVER CHANGES USING OPEN SOURCE MOLUSCE FOR LUDHIANA, PUNJAB, INDIA

Prince Dhiman*[1], Harpinder Singh[1], Nilesh Biwalkar[2], Syed Shabih Hassan[3]

*Remote Sensing & Geographic Information System, PAU, Ludhiana-141004, Punjab, India.
[1]Scientist, Punjab Remote Sensing Centre, Ludhiana-141004.
[2]Department of Soil and Water Engineering, PAU, Ludhiana-141004, Punjab, India.
[3]College of Fisheries, Guru Angad Dev Veterinary and
Animal Sciences University, Ludhiana-141004, Punjab, India

Research Article

Received: **22.07.2022** Accepted: **08.08.2022** Published: **24.09.2022**

ABSTRACT

Accurate information on land use/land cover dynamics is needed for the selection and implementation of land use programs to meet the rising demands of basic human requirements and wellbeing. Land use land cover transition analysis is a rigorous approach that helps to understand physical and human involvement in the natural environment as well as sustainable development. Thus, the study aims to predict the land use/land cover of Ludhiana, Punjab state, for the year 2033 using the MOLUSCE plugin. Classified land use/land cover maps for the years 2009, 2015, and 2020 were prepared in the Google Earth Engine platform. The prediction model used these prepared classified maps along with four generated spatial variables maps i.e. slope, elevation, distance from road, and distance from water maps. According to the study, the built-up area might grow by 85.79 sq. km between 2020 and 2033. Forecasted reductions in vegetation, bare soil, and water class cover could total 23,91, 49,02, and 12,87 square kilometers, respectively. The results may help policymakers create the best land use strategies and improved management practices of natural resources.

Keywords: Land use, Land cover, Google Earth Engine, MOLUSCE.

INTRODUCTION

Land features on the earth's surface are referred to as land use and land cover, or LULC. Land use refers to how the land is used for various purposes, such as agricultural, industrial, and residential. In contrast, land cover refers to the primary forms of land, such as towns and built-up regions, forests, water bodies, and grasslands (Meyer et al. (13)). Natural land cover has evolved into man-made land cover due to human activities to gain the essentials of everyday existence. Humans have transformed the earth's surface for several centuries, but the land cover dynamics have changed significantly with the development of new machines and techniques (Hamad et al. (6)).

Land use applications involve baseline mapping and ongoing monitoring since timely information is needed to understand how much land is now used for what purposes and to track changes in land use over time. A few instances of how human exploitation of the environment explicitly impacts the regional ecosystem are urbanization, division of agricultural land, and elimination of green spaces. This pattern of changes in LULC mainly depends on the degree of urbanization. It is crucial to identify, delineate, and map the land cover for planning, resource management, and monitoring studies.

For decision-makers and planners, understanding urban land transformation is crucial. Developing nations usually lack this information as they use conventional survey and mapping procedures that are expensive and time-consuming to estimate urban expansion. Given its affordability and technological superiority, Remote Sensing (RS) is being utilized more frequently to monitor and analyses urban

*Corresponding author: *dhimanprince.hp17@gmail.com*

growth. While using satellite image data, RS has the potential to extract information about LULC in a given area (Yuan et al. (14)).

For the design and implementation of land-use policies, information about land use and land cover dynamics is necessary to meet the growing demands of human requirements and well-being. Modelling is a solution that may be used to handle the issue of conversion and modification of LULC classes. LULC transition models often try to predict the timing and frequency of these changes. Many land cover prediction studies have been done using various statistical and analytical models. Jayasinghe et al. (7) conducted a comparative study for available urban growth prediction models. For the study, three freely available models MOLUSCE (Modules for Land Use Change Simulations), SLEUTH (Slope, Land use, Exclusion, Urban, Transport and Hillshade), and FUTURES (FUTure Urban-Regional Environment Simulation) were compared based on their prediction results for Colombo. According to their study, the FUTURES model is considered the best to simulate future urban growth. Although there are many proprietary software for LULC modelling, MOLUSCE is the most popular free and open-source option (https://github.com/nextgis/molusce). MOLUSCE combines well-known methods that can be utilized in forestry applications, urban analysis, and land use/cover change analysis. It is well suited to analyze changes in land use and forest cover over time, model possible changes in land use in at-risk areas, and simulate future changes in land use and forest cover.

Saputra et al. (10) utilized MOLUSCE module for ANN-CA (Artificial Neural Network model-based cellular automata) modeling in their study to predict LULC in North Sumatra, Indonesia. The model used five factors, including soil type, aspect, altitude, distance from the road, and slope, for the training process to examine their effects on LULC changes between 1990 and 2000, and the model predicted maps for the years 2050 and 2070. The predicted maps showed increase of about 4 percent in plantation area. By 2050, it was anticipated that the area used for farming and forests will decline by 1.2 and 1.6 percent, respectively. Kamaraj et al. (9) identified the changes in land cover in the Bhavani basin, Tamil Nadu, between 2005 and 2015. They forecasted the possible land use map for 2025 and 2030 using the MOLUSCE plugin in QGIS software. They revealed an increase of 20 km2 and 10 km2, in farmland and built-up areas, respectively. Guidigan et al. (4) aimed to examine the LULC patterns for the Benin region using MOLUSCE. They obtained land cover maps and made a simulated map for the years 2025 and 2037. The findings of this study showed a significant decrease in Savannah land and a rapid growth in agriculture and forestland.

Abbas et al. (1) used satellite imagery from 1980 to 2020, regularly at a 10-year time gap. They also used many spatial factors like distance from the road, DEM, and distance from water for integration in the MOLUSCE plugin of QGIS software to predict and analyze the simulated map of the Greater Bay Area. The study's results showed significant urban growth from 4.75 per cent to 14.75 per cent over the past 40 years. Forests regions reduced from 53.49 per cent to 50.57 per cent, farmlands areas reduced from 21.85 per cent to 16.04 per cent, and grasslands reduced from 13.89 per cent to 12.05 per cent. Alrubkhi et al. (2) aimed to see how QGIS software combined with GIS methodologies may be used to identify, assess, and analyze LULC change between 2000 and 2010, as well as predict the future of LULC. MOLUSCE plugin was used to create area change maps and to prepare a simulated future map for 2025 using cellular automata simulation. The study's results revealed a growth in the urban area but a decrease in agricultural land. The forecast also suggested that agriculture would shrink by 1.49 percent by 2025.

Nugroho et al. (8) aimed this research to map out Malang City's urban growth over 24 years and to forecast the city's future development using an ANN model and the MOLUSCE QGIS plugin for the year 2027. Maps of land information for 2003, 2009, and 2015 were classified from Landsat ETM+ and OLI. The overall accuracy of classification and kappa coefficient was about 85% and 0.76, respectively, for all obtained maps. As per the predicted map of 2027, around 1049.58 hectares of farmland and 241.29 hectares of bare land in 2015 will be converted into built-up areas accounting for an increase in the urban area of 11.79 per cent.

According to the literature study, few studies have been done on measuring and analyzing LULC of the entire Ludhiana district of Punjab state. The district has experienced significant urbanization, industrialization, and population growth during the previous few decades. Therefore, the study's objective was a) classify the satellite imagery to generate the LULC maps of 2009, 2015 and 2020 b) analyze the LULC changes and c) prepare the simulated LULC map of 2033 for the Ludhiana district.

Study area and datasets

Study Area

The district of Ludhiana is situated in the central region of Punjab state (fig. 1). The area is bounded by latitudes of 30° 33' and 31° 01' North and longitudes of 75° 25' and 76° 27' East, respectively, and is on an average 244m above mean sea level. The district's geographic area is about 3706 square kilometers. The river Sutlej forms the district's northern

boundary with the districts of Jalandhar and Hoshiarpur. The districts of Fatehgarh Sahib and Sangrur delineate the eastern and southern boundaries. In the west of the region is the district of Moga. According to the 2011 census, it has a population of around 3,498,739, making it the most populous district in the state.

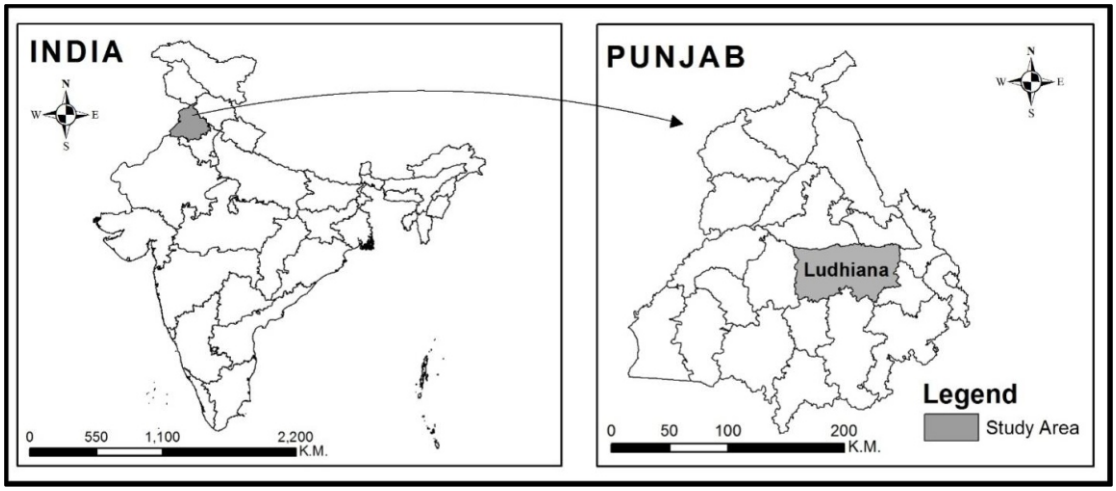

Fig. 1 Study area

Data

The atmospherically corrected surface reflectance Landsat 5 and 8 data was used for the preparation of the LULC maps of 2009, 2015 and 2020. The Landsat images courtesy of the U.S. Geological Survey, were obtained from Operational Land Imager/Thermal Infrared Sensors. These images contain five visible and near-infrared (VNIR) bands and two short-wave infrared (SWIR) bands processed to orthorectified surface reflectance, and two thermal infrared (TIR) bands processed to orthorectified brightness temperature.

The Japan Aerospace Exploration Agency (JAXA)'s free elevation dataset collection called the Advanced Land Observing Satellite (ALOS) (Tadono et al. (12)) World 3D-30m was used for the generation of slope and elevation maps. The slope, elevation, and Landsat imagery were obtained and processed in the cloud-based Google Earth Engine (GEE) platform.

Datasets regarding the major roads and water bodies (Canal network and Drainage) were sourced from the open street map (Haklay et al. (5)). These datasets were used to prepare the distance from the road, and distance from water maps. The distance from roads and water maps were processed in ArcGIS 10.4 software using the Euclidean distance tool.

Methodology

This section describes the methodology of the research work. The first step includes processing the satellite imagery and its classification for the LULC map preparation, while the second step includes the simulation and validation. GEE has been used for the first step, and QGIS and the MOLUSE plugin have been used for the second. The complete methodology of the research is presented in Figure 2.

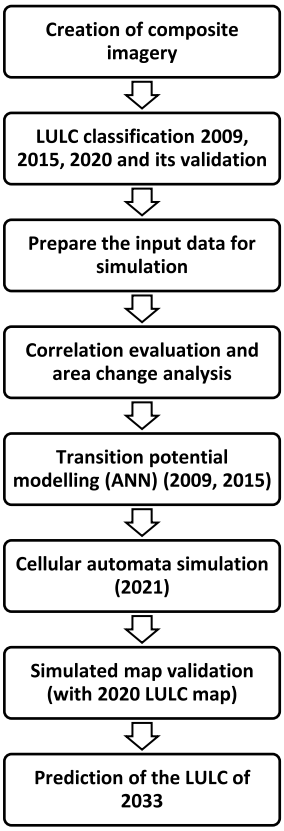

Fig. 2 Methodology

LULC Classification

Creation of composite imagery

Landsat imagery was selected for 2009, 2015, and 2020. The study used a Tier 1 surface reflectance Landsat dataset from the GEE repository. The period for filtering the imagery was selected as mid of January to the middle of February. This was done because the wheat crop was the greenest, and there was no inter-mixing of land classes during the classification. A median best composite image for a particular year was created, keeping the cloud cover percentage as low as possible. The image was further clipped for the area of interest (Fig 3).

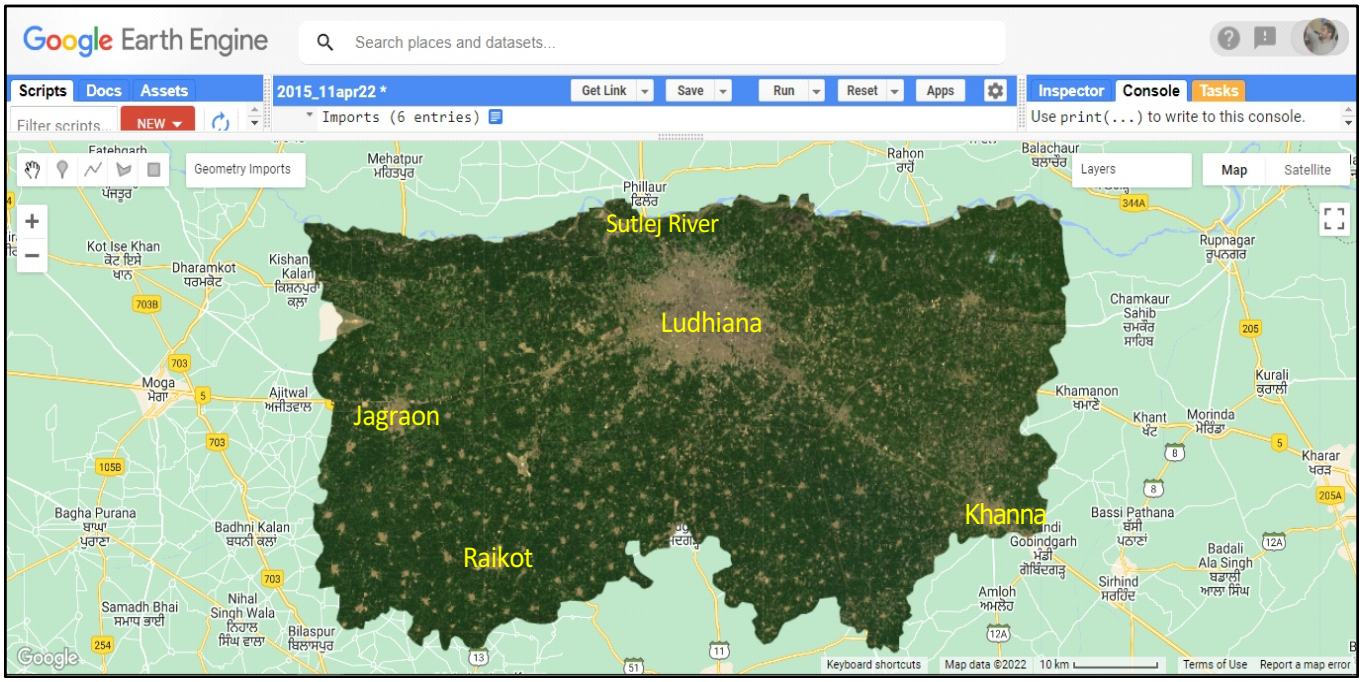

Fig 3: True Color Composite image (2015).

LULC Classification and Validation

The LULC classification was attempted on the composite imagery. LULC maps were prepared for 2009, 2015, 2020. A random forest algorithm was used for this purpose. For the classification, the imagery was categorized into four major classes (Table 1). For the preparation of the training and validation dataset for the classifier, manually ground control points (GCP) to the satellite imagery were marked for each class for various periods. Figure 4 shows various marked GCPs for the year 2015. Table 2 shows the number of GCPs marked for each imagery. The points were marked based on local knowledge and using Google Earth Pro software's time-series image visualization option. Eighty per cent of the total market points were used for the training and the remaining 20 per cent for validation purposes.

Accuracy assessment of the classified maps was done by creating a confusion matrix. The confusion matrix shows the number of pixels that were correctly or incorrectly categorized into each class. The confusion matrix was used to construct several metrics, including producer's accuracy (PA), user's accuracy (UA), overall accuracy (OA), and kappa coefficient (K). These indicators make it easier to assess the LULC classification's correctness objectively.

Table 1: LULC classification scheme.

LULC types	Description and color tone
Built-up	All infrastructures- houses, buildings, stadiums, sheds, warehouses, roads, etc. (red tone)
Vegetation	All agricultural land, forests, horticultural land, and plantations (green tone)
Bare Soil	All barren lands, vacant plots covered with shrubs, and playground grounds (yellow tone)
Water	All water bodies like rivers, canals and ponds (blue tone)

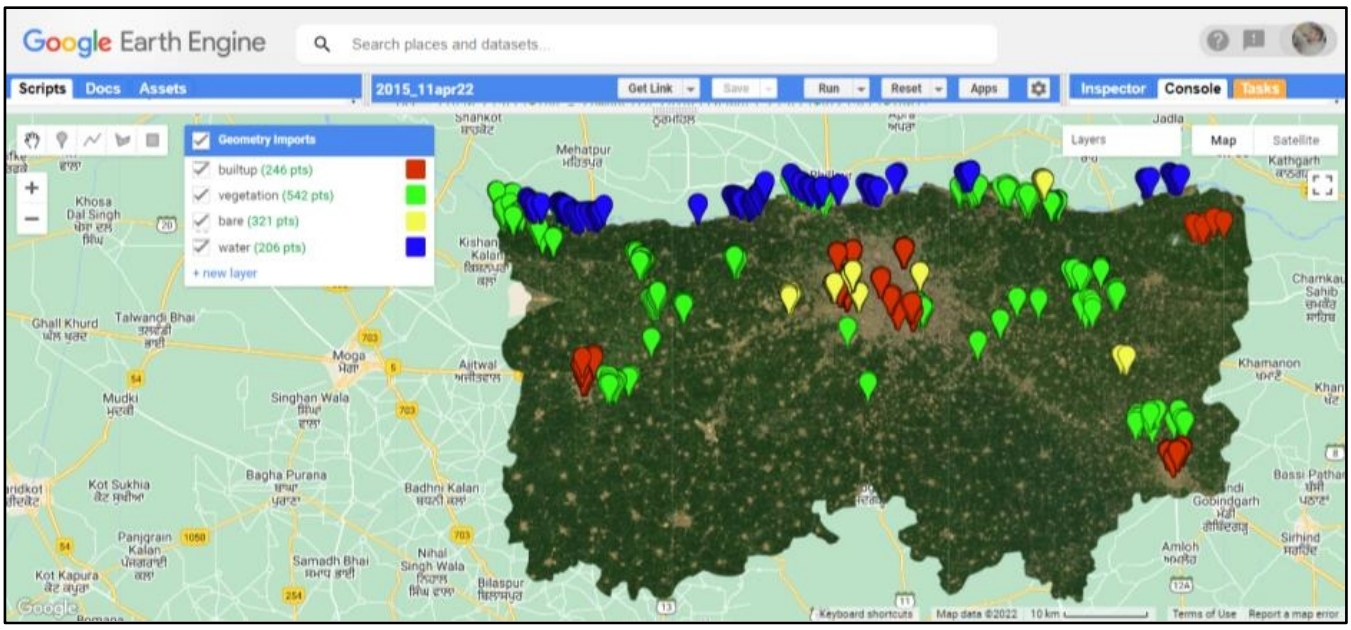

Fig 4: Marked training/validation dataset (2015).

Table 2: Number of marked training and validation GCPs

	2009	2015	2020
Built-up	238	246	463
Vegetation	432	542	526
Bare Soil	297	321	348
Water	202	206	324

Simulation

MOLUSCE plugin of QGIS software was used for the work of LULC simulation and prediction.

Input data preparation

The first step includes the input of the LULC maps for the starting year and the ending year, i.e. 2009 and 2015, respectively. Four spatial variable elements were also added: elevation map, slope map, distance from the road, and distance from water areas. The properties of the spatial variables were matched with the LULC maps before adding to the plugin. A summary of the explanatory data used in the study is shown in Table 3.

Table 3: Summary of the explanatory data used in the study.

Data	Criteria	Purpose	Source	Description
DEM	Slope	Explanatory map	ALOS JAXA	30m spatial resolution
	Elevation	Explanatory map	ALOS JAXA	30m spatial resolution
Road Map	Distance from the road	Explanatory map	OpenStreetMap	The road map of Ludhiana district
Water bodies map	Distance from the water body (Canal, Drain)	Explanatory map	OpenStreetMap	The water map of Ludhiana district

Correlation evaluation and area change analysis

Pearson's correlation was calculated to assess the geographic variable correlation among the two LULC maps and the spatial variables.

The area change analysis was done to analyze the LULC changes in the area between the initial (2009) and the final year (2015). The area change map was also generated along with the transition matrix, which shows the percentage of pixels switching between LULC classes.

Transition potential modelling

The transition probability for various classes is modelled in this stage using available methods. There are several ways to compute probable transition maps. MOLUSCE plugin offers the Artificial Neural Network (ANN), Weights of Evidence (WoE), Logistic Regression (LR), and Multi-Criteria Evaluation (MCE) approaches. Each method uses LULC change data and spatial variables as inputs for calibrating and modelling LULC changes. In this study, ANN was used to model the transition probability.

ANN algorithm works on a back-propagating learning-based iterative neural network. The neural network structure comprises three layers the input, hidden, and output. Each neuron in the output layer produces a transition probability from one form of land use to another at each cycle. By comparing the transition probability values, it is possible to predict how LULC will change from one type to another, with the highest transition probability being the new type. The corresponding cell's state is unaffected if the same type of LULC has the highest transition probability (Saputra et al. (10)).

ANN follows the below equation to calculate the transition probability:

$$P(k,t,l) = \sum_j w_{j,l} \frac{1}{1+e^{-net_j(k,t)}},$$

Where wj, l is the weight between the hidden and the output layers and P(k, t, l) is the probability of conversion from the current to the lth kind of LULC for the k-th cell at time t.

ANN model used in this study had a learning rate of 0.1, number of samples of 1000, maximum iterations of 1000 and momentum of 0.05. The optimal neural network gets stored in the memory after the learning algorithm analyses the achieved accuracy on training and validation sets of samples. Training is supposed to be completed when the highest accuracy is attained.

Cellular automata simulation

Once the transition probability has been determined, the Cellular Automata (CA) simulates the LULC. The CA simulation module provided a simulated map based on the number of iteration/s. The number of simulations should be 1 to get a simulated 2021 LULC map.

Based on four key components, the CA simulates the LULC for 2021. The components are C, n, K, and R, where C stands for pixels, n for the number of classes, K for the size of the Moore neighbourhood, and R for the transition potential maps (TPMs) (Aneesha et al. (3). In this step, the CA model identifies the 2009 and 2015 pixels with the highest TPMs values produced by transition potential modelling. This step and the transition potential modelling step are related to each other. The simulated LULC classes are created using a black box approach. The simulation resulted in a LULC map for 2021 showing the defined classes.

Validation

The MOLUSE's validation module was finally used to check and validate the simulated image of 2021. It was done using a map comparison with the classified 2020 LULC. The overall accuracy (% of correctness), kappa (overall), kappa (histo) and kappa (loc) were calculated in the end.

Once satisfactory accuracy was achieved, the simulation step of the cellular automaton to forecast future LULC was re-executed. The prediction year is determined by multiplying the iterations by the second year minus the first year. The iteration values in this study were taken as 3 for simulating the LULC of 2033.

RESULTS AND DISCUSSION

Classified LULC maps and validation

The LULC maps were prepared by classifying the Landsat satellite imagery. This study produced three 30m LULC maps of the Ludhiana district for 2009, 2015, and 2020 (Fig 4a, 4b, and 4c, respectively). Further, the confusion matrix for the classified maps was generated to validate the classified maps (Table 4). The overall accuracies of 2009, 2015, and 2020 classified maps were found to be 99.5%, 96.1%, and 95%, respectively. The kappa coefficient was also calculated for 2009 (0.994), 2015 (0.945), and 2020 (0.933). The results show that the 2009 LULC was classified with the best accuracy.

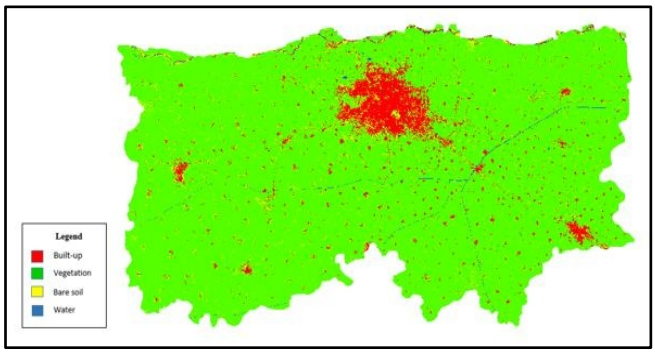

Fig. 4(a): Classified Image of 2009.

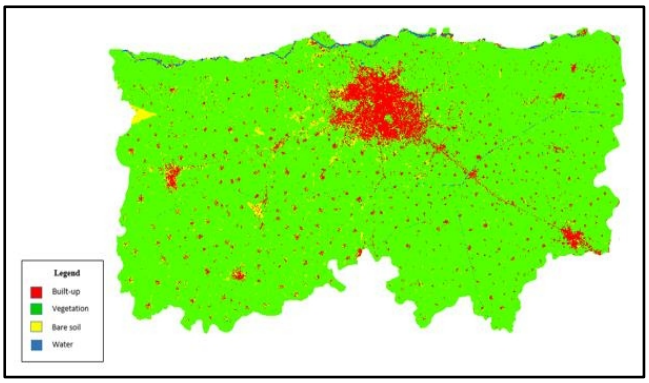

Fig. 4(b): Classified Image of 2015.

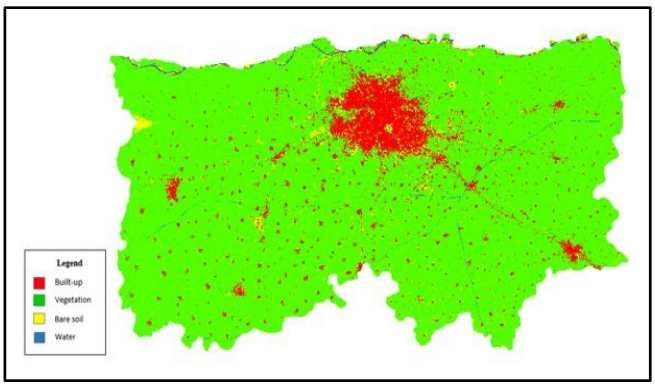

Fig. 4c : Classified Image of 2020.

Table 4 Accuracy assessment results

Year	Predicted class					PA	Overall accuracy	Kappa
	True class	Built-up	Vegetation	Bare Soil	Water			
2009	Built-up	50	0	0	0	1	0.995	0.994
	Vegetation	0	80	0	0	1		
	Bare Soil	0	1	55	0	0.982		
	Water	0	0	0	49	1		
	UA	1	0.98	1	1	-		
2015	Built-up	48	2	0	0	0.96	0.961	0.945
	Vegetation	2	100	3	0	0.952		
	Bare Soil	2	0	45	0	0.957		
	Water	0	0	0	34	1		
	UA	0.923	0.98	0.937	1	-		
2020	Built-up	92	0	2	0	0.978	0.95	0.933
	Vegetation	5	96	2	3	0.905		
	Bare Soil	1	2	63	0	0.954		
	Water	0	1	0	59	0.983		
	UA	0.938	0.969	0.940	0.951	-		

Spatial variables

Euclidean distance tool helped create distance from road and water bodies maps. Slope and elevation maps were generated from the DEM dataset in the GEE database. These spatial variables maps (Fig 5) significantly impacted the simulation model.

Area change statistics

A summary of the LULC change trend from 2009 to 2020 for each class is shown in Table 5. The increase in built-up land is noticeable and indicates an increasing trend. According to classed maps, only 196.84 sq. km., or 5.31% of the entire study region, was built-up land in 2009. 91.43% of the area was seen covered with vegetation class (3389.28 sq. km). Bare soil and water cover correspond to about the remaining 2.83% and 0.43%, respectively. In 2015, an increase of 50.64 sq. km was seen in the built-up class, accounting for 247.49 sq. km (6.67% of total area) and a decrease of 34.29 sq. km in the vegetation land (3355sq. km). Bare soil and water cover were noticed to be decreasing (Table 5). However, compared to 2015, water cover grew by 5.61 sq. km in 2020 (19.98 sq. km in total). The built-up area reached 269.37 sq. km, and vegetative land decreased to 3343.54 sq. km.

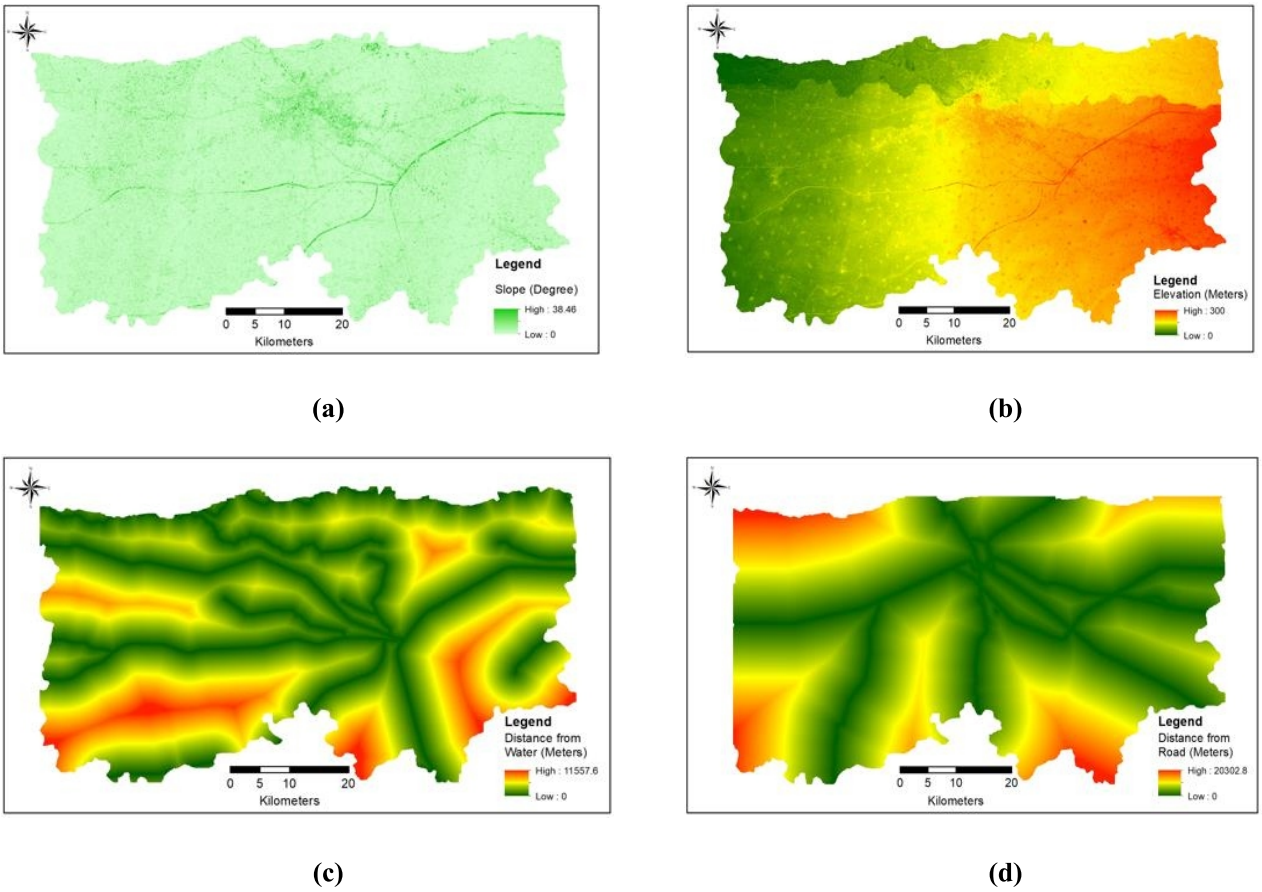

Fig. 5: Spatial variables maps (a) slope (b) elevation (c) distance from water (d) distance from road.

Table 5: LULC analysis from 2009 to 2020.

LULC Classes	2009		2015		2020	
	Area in km^2	% area covered	Area in km^2	% area covered	Area in km^2	% area covered
Built-up	196.84	5.31	247.48	6.67	269.37	7.27
Vegetation	3389.28	91.43	3355.00	90.5	3343.54	90.19
Bare Soil	104.86	2.83	90.24	2.44	74.20	2.0
Water	16.11	0.43	14.37	0.39	19.98	0.54

Simulation and its validation

With the spatial variables and the input 2009 and 2015 LULC maps, the MOLUSCE plugin's CA provided a 2021 simulated map. The simulated 2021 map was compared with the classified 2020 map to validate the CA model. The validation results showed 93.76 per cent of correctness (Fig 6) with a kappa value of 0.63. The validation results were considered good, and with the same CA model, the simulated 2033 map was generated by giving three iterations in the cellular automata simulation step. Figure 7 shows the predicted 2033 LULC map.

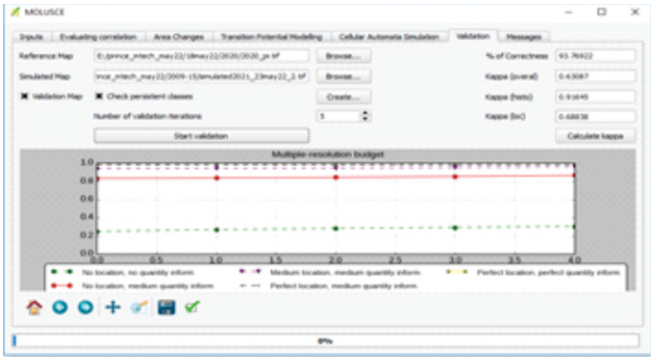

Fig. 6: Validation results.

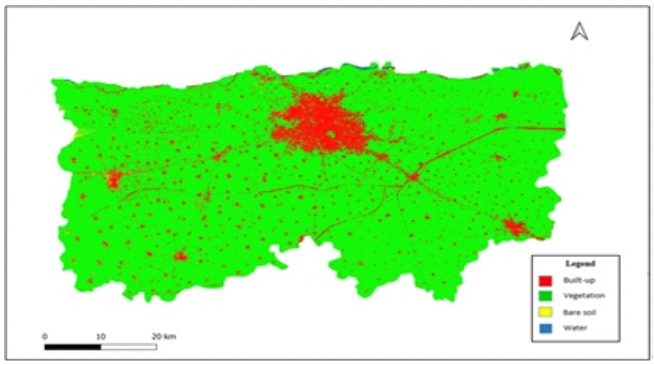

Fig. 7: Predicted LULC map (2033).

The changes in land cover classes between 2020 and predicted 2033 are presented in Table 6. Area change among the total land area was also analysed. A positive change value indicates an increase in area, whereas a negative value indicates that it has reduced. The study finds that the built-up area might increase by 85.79 sq. km in 2033 compared to 2020. The forecasted vegetation, bare soil and water class cover may reduce by 23.91 sq. km, 49.02 sq. km and 12.87 sq. km, respectively.

The study analysis revealed that generally, when one classification's area grows, the areas of other classes decrease and vice versa.

Table 6: Change in land classes between 2020 and predicted 2033.

	Class	2020	2033	Δ	2020%	2033%	Δ %
1	Built-up	269.37 sq. km.	355.16 sq. km.	85.79 sq. km.	7.26	9.58	2.31
2	Vegetation	3343.54 sq. km.	3319.63 sq. km.	-23.91 sq. km.	90.19	89.54	-0.64
3	Bare Soil	74.20 sq. km.	25.19 sq. km.	-49.02 sq. km.	2.00	0.67	-1.32
4	Water	19.98 sq. km.	7.11 sq. km.	-12.87 sq. km.	0.53	0.19	-0.34

Kalota (2015) made an effort to use landscape metrics to evaluate urban sprawl in the Ludhiana city. From 1955 to 2009, built-up areas were seen to have excessive and unplanned growth. According to the study, the city has grown rapidly due to the lack of planning and the unexpected influx of migrant labourers during the period. Most of the city's urban growth was centred in the southwest corner. According to the results, the urban area has grown dramatically and haphazardly from 1955 to 2009.

For the years 1955, 1979, 1989, 1999, 2009, and 2015, (Singh et al. (11)) calculated the annual percentage growth rates of the built class and population for the Ludhiana district. They examined that the percentage of growth rate in built-up regions was ten or more between 1955 and 1979, which fell to 6% and 4% between 1989 and 1999. The average growth rate of populated areas was noticed to be 8% overall per year.

The following studies have been conducted for Ludhiana city. Our study is for the whole district, and according to our results also, the built-up is increasing rapidly, and maximum built-up growth has been witnessed in and around Ludhiana city. A similar trend is also seen for the future.

The study's findings can be utilized as a preliminary s tep by government officials, city planners, and all other decision-makers involved in the process of preparing urban spatial planning and environmental sustainability.

CONCLUSION

Information about land use and land cover dynamics is required for the design and implementation of land-use policies in order to meet the rising demands of human needs and well-being. The prediction of LULC crucially influences plans for balancing pressures from development, conflicting users, and conservation. Thus, the ANN-CA model in the MOLUSCE plugin of QGIS software was utilized to predict the LULC map for the Ludhiana district. Firstly, the GEE cloud platform was used to prepare the LULC maps for 2009, 2015, and 2020. The LULC maps showed good classification

accuracy, with the kappa ranging from 0.93 to 0.95. The classified maps, along with spatial variables maps viz. slope, elevation, distance from the road, and distance from water bodies, were used in the ANN-CA simulation model. The model gave 93.76 per cent of correctness results on validation. The model used 2009 and 2015 maps for predicting the 2033 LULC map. The study concludes that, compared to 2020, the built-up area might rise by 85.79 sq. km in 2033. Vegetation, bare soil, and water class cover may decrease by 23.91 sq. km, 49.02 sq. km, and 12.87 sq. km, respectively.

This type of research helps us identify specific land-use changes and predict which land use will be impacted in the future to understand potential ecological risks and biodiversity loss. However, this study does not consider other factors affecting LULC changes, such as climate, policy, regulation, or human development. Therefore, incorporating those characteristics in future research will improve the results.

Conflict of interest: The authors declare that they have no competing interests.

Acknowledgement: The authors would like to thank Punjab Remote Sensing Centre, Ludhiana, along with Punjab Agricultural University, Ludhiana for their support in this research and useful discussions.

REFERENCES

1. **Abbas Z, Yang G, Zhong Y, Zhao Y.** Spatiotemporal Change Analysis and Future Scenario of LULC Using the CA-ANN Approach: A Case Study of the Greater Bay Area, China. *Land*. 2021 Jun;10(6):584.
2. **Al-Rubkhi AN, Talal AA, Mohammed AB.** Land Use Change Analysis and Modeling Using Open Source (QGis)-Case Study: Boasher Willayat. Muscat: College of Arts and Social Science, Department of Geography, Sultan Qaboos University. 2017.
3. **Aneesha Satya B, Shashi M, Deva P.** Future land use land cover scenario simulation using open source GIS for the city of Warangal, Telangana, India. *Applied Geomatics*. 2020 Sep;12(3):281-90.
4. **Guidigan ML, Sanou CL, Ragatoa DS, Fafa CO, Mishra VN.** Assessing land use/land cover dynamic and its impact in Benin Republic using land change model and CCI-LC products. *Earth Systems and Environment*. 2019 Apr;3(1):127-37.
5. **Haklay M, Weber P.** Openstreetmap: User-generated street maps. IEEE Pervasive computing. 2008 Oct 17;7(4):12-8.
6. **Hamad R, Kolo K, Balzter H.** Land cover changes induced by demining operations in Halgurd-Sakran National Park in the Kurdistan Region of Iraq. *Sustainability*. 2018 Jul 11;10(7):2422.
7. **Jayasinghe P, Kantakumar LN, Raghavan V, Yonezawa G.** Comparative Evaluation of Open Source Urban Simulation Models Applied to Colombo City and Environs in Sri Lanka. *International Journal of Geoinformatics*. 2021 Jun 1;17(3).
8. **Nugroho AB, Hasyim AW, Usman F.** Urban growth modelling of Malang city using artificial neural network based on multi-temporal remote sensing. *Civil and Environmental Science Journal* (CIVENSE). 2018 Oct 2;1(2):52-61.
9. **Kamaraj M, Rangarajan S.** Predicting the future land use and land cover changes for Bhavani basin, Tamil Nadu, India, using QGIS MOLUSCE plugin. *Environmental Science and Pollution Research*. 2022 Feb 3:1-2.
10. **Saputra MH, Lee HS.** Prediction of land use and land cover changes for north sumatra, indonesia, using an artificial-neural-network-based cellular automaton. *Sustainability*. 2019 May 28;11(11):3024.
11. **Singh R, Kalota D.** Urban sprawl and its impact on generation of urban heat island: A case study of Ludhiana city. *Journal of the Indian Society of Remote Sensing*. 2019 Sep;47(9):1567-76.
12. **Tadono T, Ishida H, Oda F, Naito S, Minakawa K, Iwamoto H.** Precise global DEM generation by ALOS PRISM. *ISPRS Annals of the Photogrammetry, Remote Sensing and Spatial Information Sciences*. 2014;2(4):71.
13. **Meyer WB, Turner BL.** Land-use/land-cover change: challenges for geographers. *GeoJournal*. 1996 Jul;39(3):237-40.
14. **Yuan F, Sawaya KE, Loeffelholz BC, Bauer ME.** Land cover classification and change analysis of the Twin Cities (Minnesota) Metropolitan Area by multitemporal Landsat remote sensing. *Remote sensing of Environment*. 2005 Oct 15;98(2-3):317-28.